THE FRIB PROJECT – ACCELERATOR CHALLENGES AND PROGRESS*

J. Wei#[1], D. Arenius[2], E. Bernard[1], N. Bultman[1], F. Casagrande[1], S. Chouhan[1], C. Compton[1], K. Davidson[1], A. Facco[1,4], V. Ganni[2], P. Gibson[1], T. Glasmacher[1], L. Harle[1], K. Holland[1], M. Johnson[1], S. Jones[1], D. Leitner[1], M. Leitner[1], G. Machicoane[1], F. Marti[1], D. Morris[1], J. Nolen[1,3], J. Ozelis[1], S. Peng[1], J. Popielarski[1], L. Popielarski[1], E. Pozdeyev[1], T. Russo[1], K. Saito[1], R. Webber[1], J. Weisend[1], M. Williams[1], Y. Yamazaki[1], A. Zeller[1], Y. Zhang[1], Q. Zhao[1]

[1] Facility for Rare Isotope Beams, Michigan State University, East Lansing, MI 48824 USA

[2] Thomas Jefferson National Laboratory, Newport News, VA 23606, USA

[3] Physics Division, Argonne National Laboratory, Argonne, IL 60439, USA

[4] Istituto Nazionale di Fisica Nucleare Laboratori Nazionali di Legnaro, Legnaro, Italy

Abstract

The Facility for Rare Isotope Beams, a new national user facility funded by the U.S. Department of Energy Office of Science to be constructed and operated by MSU, is currently being designed to provide intense beams of rare isotopes to better understand the nuclear physics, nuclear astrophysics, fundamental interactions, and industrial and medical applications. The FRIB driver linac can accelerate all stable isotopes to energies beyond 200 MeV/u at beam powers up to 400 kW. Key technical R&D programs include low-β CW SRF cryomodules and highly efficient charge stripping using a liquid lithium film. Accelerator-physics challenges include acceleration of multiple charge states of beams to meet beam-on-target requirements, efficient production and acceleration of intense heavy-ion beams from low energies, accommodation of multiple charge stripping scenarios and ion species, designs for both baseline in-flight fragmentation and ISOL upgrade options, and design considerations of machine availability, tunability, reliability, maintainability, and upgradability.

INTRODUCTION

The Facility for Rare Isotope Beams (FRIB), baselined as a 7-year, US$680 million construction project, is to be built at the Michigan State University under a corporate agreement with the US DOE [1]. FRIB driver accelerator is designed to accelerate all stable ions to energies above 200 MeV/u with beam power on the target up to 400 kW (Table 1). After production and fragment separation, the rare isotope beams can also be stopped, or stopped and then reaccelerated. The fast, stopped, and reaccelerated rare isotope beams serve a vast range of scientific users in the fields of nuclear physics and applications.

As shown in Figure 1, the driver accelerator consists of Electron Cyclotron Resonance (ECR) ion sources, a low energy beam transport containing a pre-buncher and electrostatic deflectors for machine protection, a Radiofrequency Quadrupole (RFQ) linac, linac segment 1 (with Quarter-wave Resonators (QWR) of β=0.041 and 0.085) accelerating the beam up to 20 MeV/u where the beam is stripped to higher charge states, linac segments 2 and 3 (with Half-wave Resonators (HWR) of β=0.29 and 0.53) accelerating the beam above 200 MeV/u, folding segments to confine the footprint and facilitate beam collimation, and a beam delivery system to transport to the target a tightly focused beam. The reaccelerator (ReA) consists of similar β=0.041 and 0.085 accelerating structures [2].

Table 1: FRIB driver accelerator primary parameters.

Parameter	Value	Unit
Primary beam ion species	H to ^{238}U	
Beam kinetic energy on target	> 200	MeV/u
Maximum beam power on target	400	kW
Macropulse duty factor	100	%
Beam current on target (^{238}U)	0.7	emA
Beam radius on target (90%)	0.5	mm
Driver linac beam-path length	517	m
Average uncontrolled beam loss	< 1	W/m

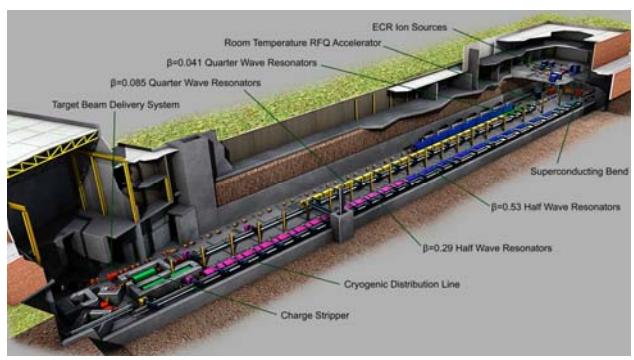

Figure 1: Layout of the FRIB driver accelerator.

*Work supported by the U.S. Department of Energy Office of Science under Cooperative Agreement DE-SC0000661
#wei@frib.msu.edu

DESIGN PHILOSOPHY

Full-energy linac technology is chosen to deliver primary beam that can meet the FRIB requirements of rare-isotope productivity and separation accuracy. Up to 400 kW of beams are focused to a diameter of 1 mm (90%), energy spread of 1% (95% peak-to-peak), and bunch length of < 3 ns (95%) on the target.

In contrast to high-intensity spallation neutron sources and neutrino sources that require pulsed beams, most of FRIB experiments prefer high-duty or continuous-wave (CW) beams. By choosing CW acceleration, a low beam current (< 2 mA) can generate the required beam power of 400 kW. Except for the ion source, effects of space charge are mostly negligible.

Superconducting (SC) technology is the energy-efficient choice for the CW linac. SC acceleration of heavy-ion beams is feasible from very low energy (500 keV/u) with practically sized cavity bores by housing both the cavities and solenoids in a cryomodule. A two-cell scheme is chosen throughout the entire linac providing both efficient acceleration and focusing. Developments of digital low-level RF control and solid-state RF amplifier technologies have made individual cavity powering and control reliable and cost efficient.

Furthermore, high availability, maintainability, reliability, tunability, and upgradability are especially required for the FRIB accelerator to operate as a national scientific user facility.

- Availability: The accelerator is designed with high beam-on-target availability accommodating normal, alternative, and fault scenarios. In the normal scenario, a liquid lithium stripper is used to raise the average charge state of ^{238}U beam to 78+ for efficient acceleration. Alternatively, helium gas confined by plasma windows with differential pumping can be used to strip the ^{238}U beam to a lower average charge state of 71+. Fault scenarios include the situation when superconducting (SC) cavities underperform by up to 20% of the design gradients. Furthermore, key components (e.g., QWR cryomodules) and subsystems (e.g., machine protection) are implemented with spares and design redundancies.
- Maintainability: The average uncontrolled beam loss is limited to below 1 W/m level for all ion species from proton to uranium, to facilitate hands-on maintenance. For a proton beam at high energy, this level corresponds to an average activation of about 1 mSv/h measured at a distance of 30 cm from the beam chamber surface, 4 hours after operations shutdown [3]. For heavy ions like uranium at low energies, activation and radiation shielding is of less concern; the 1 W/m limit addresses concerns in damage on superconducting cavity surfaces and in cryogenic heat load. To facilitate maintenance of individual cryomodules, warm interconnect sections are used between cryomodules, and U-tubes with bayonet connections are used for cryogenic distribution (Figure 2).
- Reliability: A Machine Protection System (MPS) minimizes component damage and operational interruption (e.g. magnet quench and cryogenic load increase) caused by both acute (fast) and chronic (slow) beam losses. Upon acute beam loss, the MPS response time is 35μs (including diagnostics, signal processing, and residual beam dumping). MPS responding to slow beam loss is complicated by low sensitivity of conventional ion chamber loss detection to low-energy heavy ions and beam-loss signal background from adjacent linac segments with which beam energies are significantly different. Beam-halo- scraping rings in the warm interconnect sections and possible thermal sensors at cold regions are planned for more sensitive loss detection [4].
- Tunability: The accelerator is designed to be easily tunable during both beam commissioning and operations [5]. In linac segment 1, where beam transverse-phase advance is large, cold beam-position monitors (BPM) are implemented in the cryomodules. Efforts are made in establishing beam-tuning strategies based on virtual accelerators and on-line models under normal and fault conditions.
- Upgradeability: Space is reserved in linac segment 3 to house another 12 cryomodules to readily increase the energy of ^{238}U beam above 300 MeV/u. If cavities with 35% higher accelerating gradient are used in linac segments 2 and 3, the beam-on-target energy can be raised above 400 MeV/u for ^{238}U. The linac tunnel allows future expansion so that a dedicated light-ion injector can be added supporting rare isotope production using the isotope separation on-line (ISOL) method [1]. Using an RF deflector cavity and a Lambertson septum magnet, $^{3}He^{+}$ beam supplying protons to the ISOL target can share cycle with the ^{238}U beam feeding the fragmentation target; thus simultaneous users are supported. Furthermore, space is reserved to house instrumentations including non-destructive diagnostics and sub-harmonic (e.g. 20.125 MHz) buncher that are compatible with future user demands of experiments.

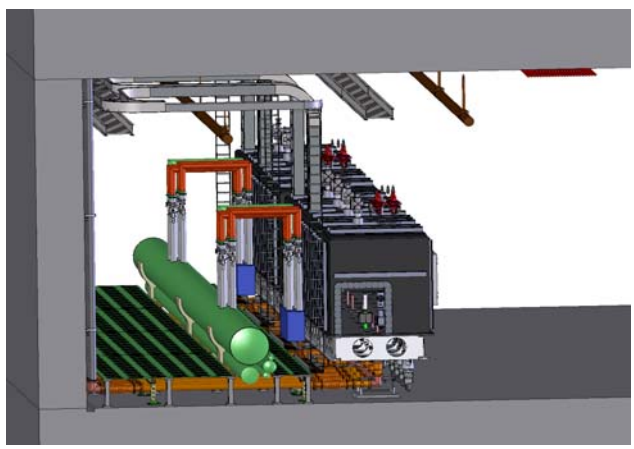

Figure 2: Layout of cryomodule inside FRIB driver accelerator tunnel showing U-tube cryogenic connections.

ACCELERATOR PHYSICS CHALLENGES

The FRIB accelerator design combines the complexity of heavy ion accelerators with the engineering challenges of high-power accelerators [3]. Due to the low charge-to-mass ratio, heavy ion acceleration is often not efficient. Uncontrolled beam loss, which usually is not an issue for low-power heavy ion machines, is of primary concern for the FRIB accelerator. Comparing with high-power proton machines like the Spallation Neutron Source (SNS) linac where apertures of the elliptical SC cavities [6] are large and beam amplitude reaches maxima in the warm locations of the focusing quadrupole magnets, the apertures of the FRIB QWR and HWR accelerating structures are small and beam amplitude reaches maxima in the cold solenoid locations inside cryomodules. Requirements on beam halo prevention, detection and mitigation are stringent.

To maximize beam intensity on the target, beams of multiple charge states are accelerated simultaneously (2 charge states of 33+ and 34+ before stripping, and 5 charge states of 76+ to 80+ after stripping for ^{238}U). Bends of second-order achromatic optics are used to fold the beams, and cavity phases are adjusted so that beams are longitudinally overlapping at the charge stripper [7].

Conventional charge strippers like solid carbon foils are not sustainable at the power of a ^{238}U beam at 17 MeV/u during normal operations [8]. FRIB accelerator lattice needs to accommodate beam acceleration of different charge states resulting from various stripping methods including liquid lithium and helium gas (average charge state from 63+ to 78+ for ^{238}U). Buncher cavities of fundamental (80.5 MHz and 322 MHz) and double (161 MHz) linac RF frequencies are strategically placed in the folding segments to preserve beam quality.

Due to the short stopping distance in surrounding materials, uncontrolled beam loss of the low-energy heavy ions can cause damage to the surface of accelerating structures much more easily than a proton beam. On the other hand, due to the low level of radio-activation [9], losses of low-energy heavy-ion beams are difficult to detect [4]. Beam-loss detection and machine protection often rely on beam scraping. On the other hand, scraping of partially stripped ions may lead to higher ionization further complicating beam collimation and machine protection [10].

Due to requirements of frequent longitudinal and transverse focusing in the superconducting acceleration structure, focusing solenoids are placed inside cryomodules adjacent to cavities. Alignment tolerance of these solenoids is ±1 mm under cryogenic conditions. Horizontal and vertical steerers are needed to thread the beam and correct the beam orbit.

Stringent beam-on-target requirements demand tight optical control, error control, and advanced beam diagnostics. The primary beam of 400 kW needs to be focused into a diameter of 1 mm with below ±5 mrad transverse angular spread. The desired range of beam power variation on target is 8 orders of magnitude. Orbit stability needs to be controlled at 0.1 mm level.

TECHNOLOGY CHALLENGES

Major R&D topics of FRIB accelerator systems include high-efficiency charge stripping and superconducting RF technologies for low-β acceleration.

Charge Stripper

The FRIB baseline design of charge stripping [11] was based on the ANL work on a liquid-lithium high-power thick target where it was demonstrated power deposition of 20 kW (from an electron beam) with the liquid lithium operating well in an accelerator environment. During the last couple of years the stability of a thin liquid film with the correct thickness for the FRIB stripper (~600 μg/cm^2) was achieved (Figure 3). The next step is to show that the power deposited by the primary beam on the moving film (~ 1 kW) will not destroy or perturb it. With this purpose we borrowed the LEDA ion source and LEBT from LANL and plan to modify the optics to obtain a 1 to 3 mm diameter beam spot on the liquid-lithium film. As the protons will stop on the film the power will be comparable to the power deposited by the heavy ions during operation. The source reconfiguration is taking place at MSU. Once the new optics is checked on a new platform that is matched to the ANL lithium loop, the device will be moved to ANL for the integrated test.

A second option for the stripper consisting of a helium gas cell enclosed by plasma windows was considered. The RIKEN group has shown [12] that helium gas produces a higher average charge state than a nitrogen gas stripper. The purpose of the plasma windows is to limit the helium gas leaking out of the gas cell [8].

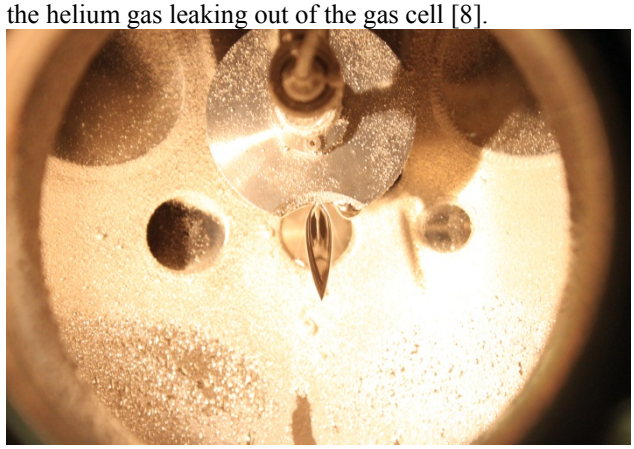

Figure 3: Liquid lithium film established at ANL.

Superconducting RF

FRIB driver linac is the first full-size SC linac using a large quantity (340) of low-β cavities. Cavity design is optimized not only for optimum performance but also for low production cost [13]. This requirement guided the choice of the cavity geometries, materials and mechanical solutions, avoiding complicated shapes, minimizing the amount of electron beam welds, eliminating bellows, optimizing construction and surface treatment procedures. FRIB cavities work with superfluid helium at 2 K. The increase in cavity Q more than compensates the loss of efficiency of the 2 K cryogenic system. This innovative

choice in a low-β linac allows operation of cavities in stable pressure conditions with high safety margin on the maximum surface fields.

Cavity Development. After a 10-year development, the 2nd generation QWR prototypes are used in the ReA3 linac (7 with β_0=0.041 in operation and 8 with β_0=0.085 under installation). This cavity type underwent modifications including the displacement of the RF coupler from the bottom plate to the resonator side and an increased distance between the tuning plate and the inner conductor tip, in order to remove a critical thermal problem in the design. The new tuning plate includes slots and undulations to increase its maximum elastic displacement and thus its tuning range, and a "puck" whose length can be adjusted for cavity tuning before final welding. Concerning the β_0=0.53 HWR prototype, which is similar in design to the β_0=0.29 cavity, 4 units of the 2nd generation have been built by 2 different vendors in addition to the one built in house. After positive test results, the β_0=0.085 QWR and the HWRs designs have been further refined in a 3rd generation, upgraded design with increased diameter that takes maximum advantage of the space available in FRIB cryomodules (Figure 4 and Table 2) [14].

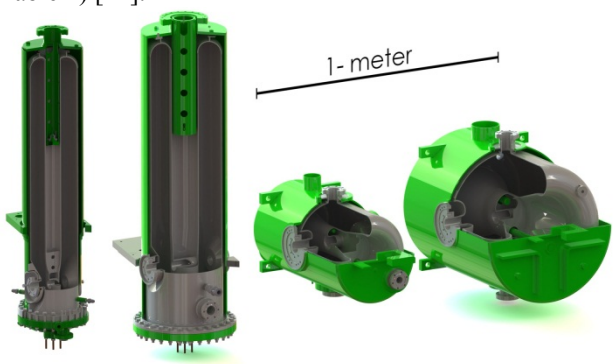

Figure 4: FRIB SC cavities. From left: β_0=0.041 and 0.085 QWRs, β_0=0.29 and 0.53 HWRs.

Table 2: Upgraded FRIB cavity parameters

Resonator	QWR1	QWR2	HWR1	HWR2
β_0	0.041	0.085	0.29	0.53
f (MHz)	80.5	80.5	322	322
V_a (MV)	0.81	1.8	2.1	3.7
E_p (MV/m)	31	33	33	26
B_p (mT)	55	70	60	63
Q_0 (10^9)	1.2	1.8	5.5	7.6
R/Q (Ω)	402	452	224	230
G (Ω)	15	22	78	107
Aperture (mm)	34	34	40	40
$L_{eff} \equiv \beta\lambda$ (mm)	160	320	270	503
Number of cavities	12	94	76	148

Surface Treatments. Test results and production cost considerations led to the choice of buffered chemical polishing (BCP) for FRIB cavity's surface treatment. The effort was concentrated in the development of a reliable procedure [15] able to produce field-emission free, high gradient cavities. The treatment includes the following BCP steps: 1) bulk etch (~150μm removal), 2) differential etching in QWRs for final cavity tuning if required, 3) light etch (~30 μm removal). Thermal treatment in high vacuum at 600 °C is applied before step 3) for Hydrogen removal to prevent Q disease. High pressure water rinsing (HPR) is applied before cavity final installation. To assure surface cleanliness, dust particle count is performed on resonator surfaces during cavity assembly in the clean room and the water purity is continuously monitored during HPR. During BCP both the cavity and acid temperatures are stabilized to control the removal rate and to avoid excess of hydrogen absorption in Nb. The acid flow path in the β_0=0.53 HWR was studied by means of simulations and experiments to obtain homogeneous removal over the entire inner resonator surface. Final thermal treatment at 120°C was also implemented, showing significant reduction of the Q-slope at 4.2 K, but negligible improvement at 2 K.

Test Results in Prototypes. The 2nd generation prototypes of β_0=0.085 QWR and 0.53 HWR have been tested in vertical dewars at 2 K exceeding FRIB design specifications (Figures 5 and 6) [14].

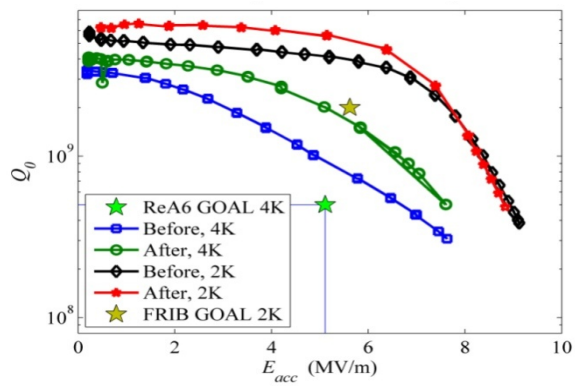

Figure 5: ReA3, β_0=0.085 QWR prototype Q_0 vs. E_{acc} at 2 K and 4.2 K, before and after 120°C baking.

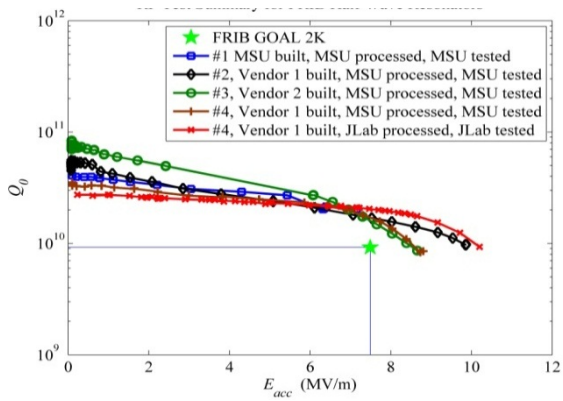

Figure 6: Performance of the β_0=0.53 HWR prototypes Q_0 vs. E_{acc} processed and tested at MSU and JLAB.

The residual resistance measured in the prototype families was below 5 nΩ up to about 100 mT in QWRs, and about 80 mT in HWRs. Considering that the FRIB specified limits are 11 nΩ and 70 mT, a large safety margin exists for future upgrades (Figure 7).

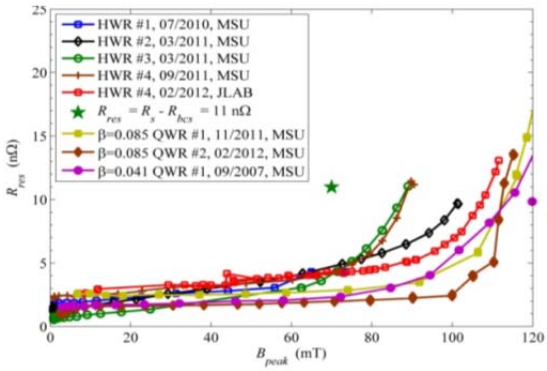

Figure 7: Residual surface resistance at 2 K of β_0=0.041 and 0.085 QWR and β_0=0.53 HWR prototypes.

Design Upgrade. The 3rd-generation cavity design optimization resulted in significant improvement of peak fields E_p/E_{acc}, B_p/E_{acc} and shunt impedance R_{sh}, with consequent reduction of the overall linac cost and operational risk. E_p and B_p in operation could be moved below the safe values of 35 MV/m and 70 mT in all cavities. The design gradients of the β_0=0.085 QWR and β_0=0.29 HWR are raised by 10% without increasing the total cryogenic load, allowing a reduction of two cryomodules. The apertures of all QWRs were enlarged from 30 to 34 mm, and their bottom rings were modified for efficient tuning-plate cooling using a low-cost design [14]. The HWR designs were optimized to facilitate the mechanical construction and tuning procedure. In all cavities, the helium vessel is made of titanium to avoid brazed Nb-to-stainless-steel interface.

Figure 8: TDCM containing two β_0=0.53 prototype HWR and a solenoid during installation in the test bunker.

β_0=0.53 Prototype Cryomodule (TDCM). The Technology Demonstration Cryomodule (TDCM) consists of two β_0=0.53 HWRs operating at 2 K and a 9 T solenoid operating at 4.5 K arranged in a "top-down" configuration (Figure 8). The cryomodule was tested at the design cryogenic temperatures demonstrating excellent cryogenic and LLRF control stabilities. Multipacting was found to impede the performance of the cavities and the coupler. Future tests are planned starting August 2012 on magnetic field and shielding studies, mechanical-type and pneumatic-type tuner evaluations, multipacting mitigation, and integrated tests with both β_0=0.29 and β_0=0.53 HWRs.

ACCELERATOR DESIGN

The FRIB facility is designed adjacent to the ReA facility [2] to benefit fully from the existing experimental infrastructure at the National Superconducting Cyclotron Laboratory (NSCL) (Figure 9). The driver linac is folded twice to minimize the footprint impact on campus, and the tunnel layout allows "open cutting" to save on civil construction costs. Design of the penetrations between the tunnel and the service buildings is compatible with the planned energy upgrade. Space is reserved to house kickers, septums, and target of a future ISOL facility and "stubs" are built to the tunnel walls to allow connection to a future light-ion injector for the planned upgrades.

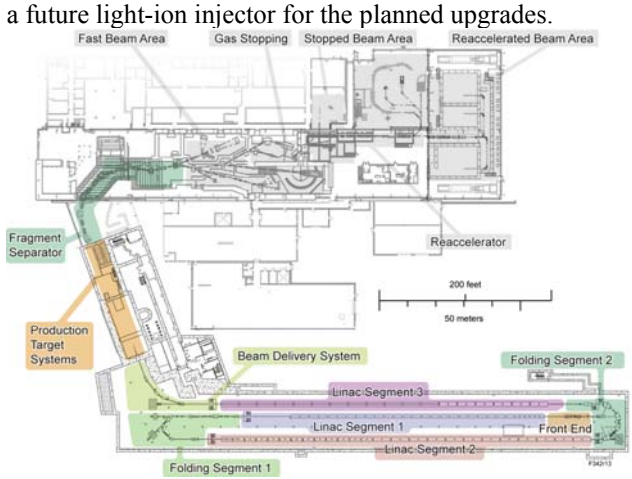

Figure 9: Layout of the FRIB facility (colored) at MSU.

Front End

The FRIB Front End includes two ECR sources (ECRIS), two charge selection systems, a LEBT, a RFQ, and a MEBT (Figure 10). To enhance availability and maintainability, placed at the ground level in the support building about 10 m above the tunnel level are two ECR sources: a SC high-power source based on the SC ECRIS VENUS developed at LBNL [16] and, initially, a room-temperature ECRIS ARTEMIS available at NSCL.

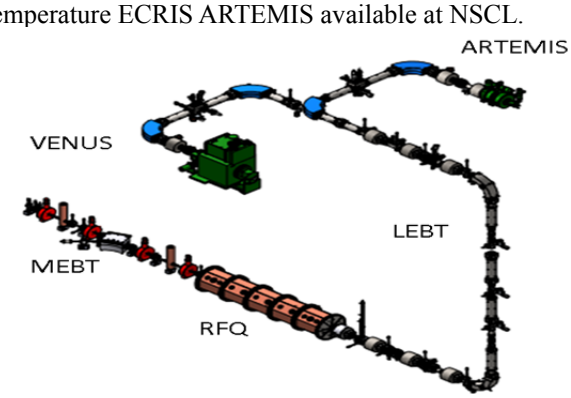

Figure 10: FRIB Front End with its major subsystems.

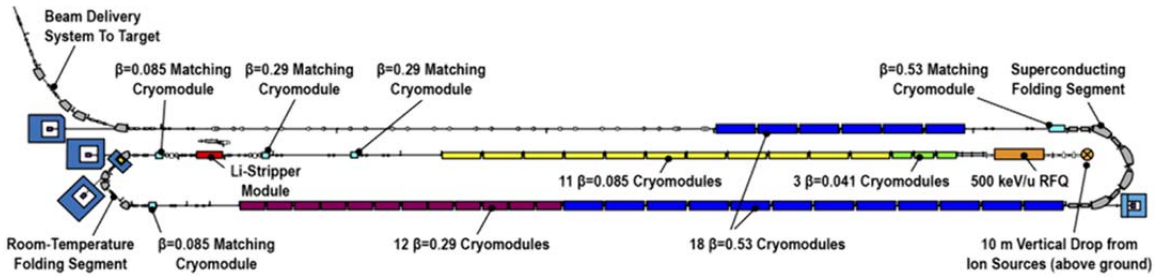

Figure 11: Layout of the FRIB driver accelerator at the tunnel level.

The beams extracted from the sources are filtered in the charge selection systems. The LEBT design is achromatic allowing transporting two charge states simultaneously to double the accelerated beam intensity. To facilitate transport of the two-charge state beams the LEBT uses electrostatic quadrupoles and two 90° dipole deflectors in the vertical transport line. To reduce losses in the superconducting linac, the beam is collimated by several apertures in the LEBT. Then, the CW beam is bunched by a multi-harmonic buncher operating at 40.25, 80.5, and 120.75 MHz before injection into the RFQ. A second RF cavity operating at 40.25 MHz upstream of the RFQ is required for two-charge-state beam injection acting as a velocity equalizer and reducing the longitudinal beam emittance. A chopper is used to vary the duty cycle controlling the pulse length from several hundreds of ns to CW and the pulse frequency from 0 to 30 kHz. Several mesh screens allow reduction of the beam intensity by several orders of magnitude while keeping the nominal bunch frequency. The two 90° electrostatic deflectors in the vertical transport line are incorporated into the machine protection system. The voltage on the deflector plates with shut-off time below 1 μs are controlled by fast switches that receive the inhibit signal from the MPS.

The RFQ accelerates the beam from 12 to 500 keV/u. Downstream of the RFQ, the MEBT consists of two room-temperature QWR bunchers, four SC solenoids, an energy analyzing dipole, and diagnostics. It matches the beam to the SC linac and removes un-accelerated beam that is not longitudinally captured in the RFQ.

Linac Segments

Three sequential linac segments (LS1, LS2, and LS3), each over 100-m long, accelerate the beam from 500 keV/u to above 200 MeV/u (Figure 11). There are 44 acceleration cryomodules and 5 rebuncher cryomodules in the linac containing a total of 330 QWR and HWR cavities. 9-T SC solenoids provide beam transverse focusing in all the acceleration cryomodules. In order not to quench adjacent SC cavities, buckling coils are equipped with each solenoid to limit the stray fields. Meanwhile, residual magnetic fields are limited to no more than 15 mG to ensure SRF performance of the cavities. Along with cryomodule magnetic shielding, an automatic degaussing process is designed for the SC solenoid.

Several potential "hot spots" are likely to compromise SRF performance: ion source, charge stripper, charge selector, and fragment target. Fast acting valves of ms response time are designed at both ends of each linac segment to protect cryomodules against vacuum failures.

Since energy gains in the cavity are different for beams of different charge states, a multi-reference-particle model is established to handle various charge states of respective beam trajectory, beam energy, synchronous phase, focal length and phase advance. Transverse coupling in a lattice containing solenoids presents another challenge to beam matching even though the beam is nominally round. Particle tracking simulation with 3D fields indicates that even if a round beam is injected into the linac, it will become tilted in the linac presumably due to the quadrupole components of the QWR cavities. Transverse matching of a coupled beam requires fitting of 10 variables comparing with 6 of a decoupled beam.

Folding Segments and Beam Delivery System

Two folding segments split the linac in three segments. The stripper is located just upstream of the first 180˚ bend. Four 45˚ room-temperature dipoles and several combined function (quadrupole/sextupole) magnets control the chromatic effects. Five charge states of ^{238}U are transported with different rigidities ($\Delta Q/Q \sim 3\%$). SRF rebunchers are located before and after the bend to match the longitudinal phase space to the acceptance of the second linac segment. This first bend effectively facilitates charge selection and beam halo scraping.

The second bend was introduced to reduce the tunnel footprint, as shown in Figure 11. Four superconducting dipoles of 2 T maximum field adopt similar design to the dipoles used at NSCL in the A1900 fragment separator. Afterwards, the beam is further accelerated in the third segment and then bent 70˚ toward the production target where the objective is to achieve 90% of the beam in a 1 mm diameter beam spot with all five charge states superimposed. The final component of the transport line is the final focus triplet where special care is taken to reduce the chromatic aberrations.

Reaccelerator

The re-accelerator facility (ReA) is a heavy ion linac consisting of an Electron Beam Ion Trap (EBIT) charge breeder, an off-line stable ion beam injector, a multi-

harmonic buncher, an RFQ, and 8 cryomodules (one β_o=0.041 cryomodule, four β_o=0.085 cryomodules, and three bunchers) with a total of 41 SC cavities. ReA reaccelerates the rare isotope ion beam after it was mass-separated in the fragment separator and decelerated to thermal energies. The 1+ rare isotope beam is injected into an EBIT charge breeder, stripped to a Q/A between 0.2 and 0.5 and accelerated in the linac. ReA is designed to provide beams with energies from 0.3 to 12 MeV/u for heavier ions and from 0.3 up to 20 MeV/u for light ions.

The first stage of ReA (ReA3) is partly under beam commissioning. The first two β_o=0.041 cryomodules were installed in 2010 and commissioned in 2011. The third cryomodule (β_o=0.085) is planned to be installed by the end of 2012 completing the ReA3 project. In 2014 an additional β_o=0.085 cryomodule will be added which will enable acceleration of all ions above the Coulomb barriers. A limited user program utilizing rare isotopes produced by the Coupled Cyclotron Facility (CCF) is scheduled to start in 2013.

During the commissioning of the cryomodules, the stabilities of SRF cavities and LLRF control were successfully demonstrated to FRIB requirements [2]. Figure 12 shows the first beam energy spectrum observed in ReA3 during commissioning with a He^+ beam. Each peak corresponds to a beam energy shift after the RFQ when each cavity is sequentially turned on and phased for acceleration at nominal ReA3 gradients (V_a=0.432MV). In addition, the first 1+ to n+ acceleration using the EBIT charge breeder was recently demostrated. For this test, a single charged ^{39}K beam was injected into the EBIT source from the off-line test source, charge bred to 16+ and accelerated through the linac.

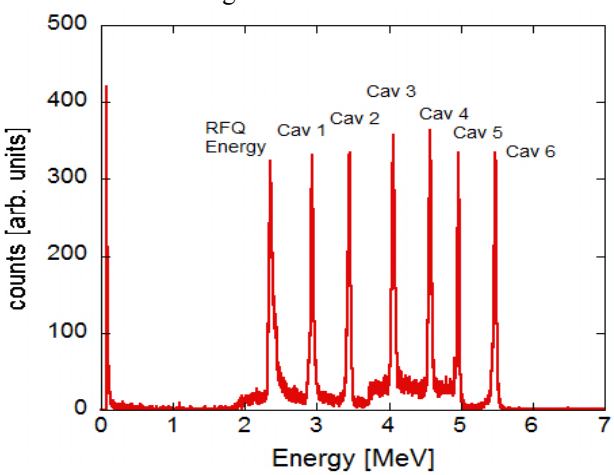

Figure 12: Energy spectra measured with a silicon detector. By turning on one cavity at a time the nominal final energy of 5.486 MeV (1.38MeV/u) was reached.

SUBSYSTEM DESIGN & ACQUISITION

Design & Acquisition Strategy

After the project baseline, the FRIB project entered into its final design phase when detail engineering designs are performed at MSU. While critical processing and assembly are planned to be performed in house, fabrication of a large quantity of repetitive components are planned through mass production and out-sourcing by industrial providers. Based on quoting and purchasing experiences, a cost reduction of 2 to 3 times is expected between prototypes and mass-produced items.

The FRIB project plans to place approximately 450 procurements valued at more than $50k each. The sum of all technical equipment procurements amounts to $217M excluding conventional facility construction. We have implemented a procurement strategy that strives to reduce vendor risks for the best value to the FRIB project:

- We work directly with the vendors understanding their individual risk concerns and proposing mitigations:
  - Perform certain tasks in-house if the vendor lacks capability;
  - Adjust engineering designs to allow vendor to implement familiar fabrication approaches;
  - Identify key-personnel bottlenecks at the vendor, and provide technical support where necessary;
  - Work closely with the vendor in mass-production planning and subsequent quality monitoring;
  - Accept components on mechanical (dimensional) properties instead of functional (e.g. electromagnetic, RF) performance;
  - FRIB to purchase high-cost materials that expose to market fluctuations (e.g., Nb).
- We evaluate how the project fits into the supplier's total capabilities and long-term business plans to gauge supplier management's commitment to solve production challenges and risks.
- We develop long-term supplier relationships for mass production. Phasing of procurements from prototypes to production sensitizes vendors to be able to successfully produce the unique components.

So far we have implemented this strategy to negotiated favorable prices for all the SRF material purchases and the production of 174 β=0.53 HRWs [17].

Cryogenics

The cryogenics system is designed to support the operation of both SC cavities at a sub-atmospheric pressure (2 K) and SC magnets at a pressure slightly over atmospheric. The system must also provide a 4.5 K liquefaction load to support the magnet's power leads and a non-isothermal refrigeration-shield load between 38 and 55 K. Table 3 summarizes the interface heat load requirements for each load temperature.

The distribution system consists of three separate linac-segment lines and a separator-area distribution line. It uses cryogenic disconnects consisting of vacuum insulated "U-tubes" and bayonets integrated with non-cryogenic isolation valves that are similar to JLab and SNS designs. Each segment, as well as individual cryomodules, may be cooled down and warmed up independently.

The options to support various cryomodule loads are described and evaluated in [18]. The number and location

of valves and interface locations between distribution system and cryomodules are considered to accomplish cool down, warm up, and isolation, as well as for efficient and steady operations.

Since the dominant refrigeration load is at 2 K, the refrigeration process is based on the process options study presented in [19] and incorporates the cumulative experience from both JLab and SNS cryogenic systems. Since the load estimates are approximate, margins are included in these load estimates for the refrigerator. The recent experience gained from the JLab 12 GeV cryogenic system design is utilized for both the refrigerator cold box and the compression system designs. The Floating Pressure Process – Ganni Cycle [20] is to be implemented to provide efficient adaptation to the actual loads.

Table 3: Interface Load Requirements. In addition, the total magnet lead flow is 3.2 g/s, representing 3% of the total load exergy.

Source	Heat load [W]		
	2 K	4.5 K	38 – 55 K
Cryomodule	2490	1470	7690
Magnets	0	670	1000
Cryodistribution	0	950	5000
Beam loss	0	25	0
Total load	2490	3115	13690
Load exergy fraction	54%	30%	13%

Cryomodule

After the conceptual design, the FRIB cryomodule design has evolved significantly from the "top-down" ReA3 style to a "bottom-up" design. Key features including rail system, support system, heat and magnetic shields are simplified along with improvements in assembly and alignment. Figure 13 shows the current design incorporating a torque-resistant structural frame made of stainless steel. We incorporate machined fiberglass compression posts supporting the coldmass in the cryomodule vacuum vessel. Three posts on linear roller bearings oriented towards the center of thermal contraction serve as 6-degree-of-freedom kinematic supports. This design controls the alignment of the coldmass while allowing thermal contraction. Cavity and solenoid attachment points to the rails are all machined after welding to ensure assembly consistency [21].

The FRIB cryomodules contain separate cryogenic circuits at 4 K for the solenoids and at 2 K for the cavities with the 2 K heat exchanger residing inside. We are currently evaluating cavity operation at 2.1 K. The slight reduction in cavity Q would be offset by substantial savings in cryoplant costs. However, care must be taken for quiescent cavity operation close to the helium λ-point.

The project schedule calls for a production rate of 2 cryomodules per month. Cavity processing, vertical tests and coldmass assembly are planned to be performed in-house. The cryomodule thermal shield, magnetic shield, cryogenic plumbing, and vacuum vessel will be procured from industry as complete "plug-in" units ready for assembly in the cryomodules.

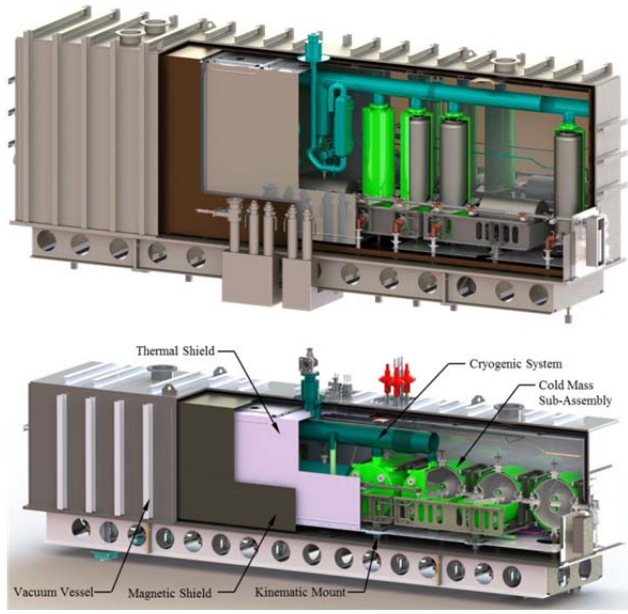

Figure 13: FRIB "bottom-up" cryomodule designs. The top cryomodule incorporates 8 β=0.085 QWRs, 3 solenoids, and 3 cold beam position monitors; the bottom cryomodule incorporates 8 β=0.53 HWRs and a solenoid.

RF

The RF System monitors and controls the amplitude and phase of the voltage in the cavities. The RF System consists of the reference clock generation and distribution line, LLRF controllers, RF amplifiers, RF transmission lines including couplers and pickup cables, cavity spark detectors, and cavity tuner controls (Figure 14).

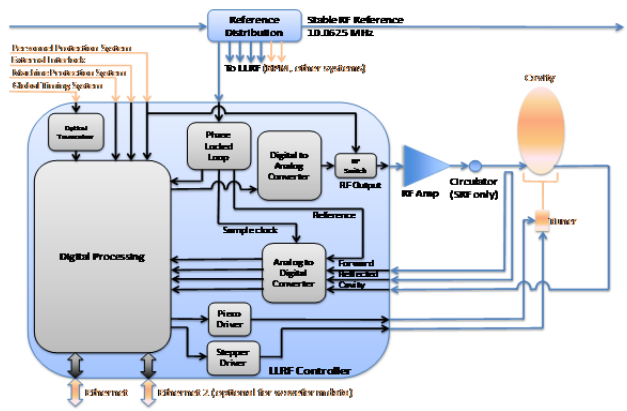

Figure 14: RF system interface block diagram.

The RF Reference clock is generated by a 10.0625 MHz oven-controlled crystal oscillator and distributed along the linac via phase-stabilized RF cable with temperature variation below ±5ppm/˚C. The reference line has directional couplers near each cryomodule. The

reference signal cable from the directional coupler to the LLRF module in the service building is routed as close as possible to the forward, reflected, and cavity feedback signals to minimize the effects of temperature drift.

The LLRF controller directly samples the cavity feedback signals and the reference signal. The sample clock is locked to and derived from the reference clock. The sample clock frequency is chosen to minimize the aliasing effects of harmonics that may be present in the incoming signals. The raw samples are filtered and converted to phase and amplitude in the field-programmable gate array (FPGA) and control logic directly produces the output frequencies using a high-speed digital-to-analog converter (DAC). The tuner control signals are also generated in the FPGA using information from the RF feedback signals.

A new control method - active disturbance rejection control (ADRC), is applied to solve the problem of microphonics detuning in the SC cavities. ADRC provides 200% improvement over the proportional-integral-derivative (PID) method in simulations and 400% improvement in hardware tests. A digital self-excited loop mode was also implemented in the LLRF controllers.

With the exception of the RFQ amplifier (200 kW tetrode), the FRIB RF amplifiers use solid-state technology. Multiple amplifiers can be combined to generate the required power (up to 8 kW for β=0.53 HWRs). The isolation provided by the circulators allows the use of N-way power combiners which saves space and cost. The high-power RF cables, connectors, circulators, power combiners and transmission lines for the SRF amplifiers are rated to handle the standing waves produced by the reflected power due to over-coupling.

Ion Source

The ARTEMIS ECR source built at MSU based on the AECR-U design at LBNL operates at 14.5 GHz with room-temperature coils.

The VENUS-style ECR source will be a SC high-performance ECR source operating at 28 GHz. In 2007, VENUS demonstrated the FRIB current [16] for a ^{238}U beam when combining the two charges states of 33+ and 34+. Recent beam measurements demonstrated that better performances from VENUS can be obtained by coupling additional microwave power (up to 8 kW) to the ion source. A new intensity record of 450 eμA of $^{238}U^{33+}$ was obtained with VENUS at LBNL. The measured emittance for this charge state showed that 95% of the beam was within the FRIB acceptance. FRIB modifications to the original design of the VENUS cryostat include the cooling capacity at 4.2K been extended from 6 W to 12 W to include the dynamic heat load generated by the plasma Bremsstrahlung electrons.

Both sources are installed on a high-voltage platform to provide an initial beam acceleration of 12 keV/u at FRIB.

RFQ

The FRIB RFQ accelerates the multi-charge state beam from 12 to 500 keV/u over a 5-m distance with estimated transmission efficiency above 80%. It operates at 80.5 MHz and requires about 100 kW of CW RF power. A 4-vane resonator is utilized with a liner ramped accelerating voltage profile (Figure 15).

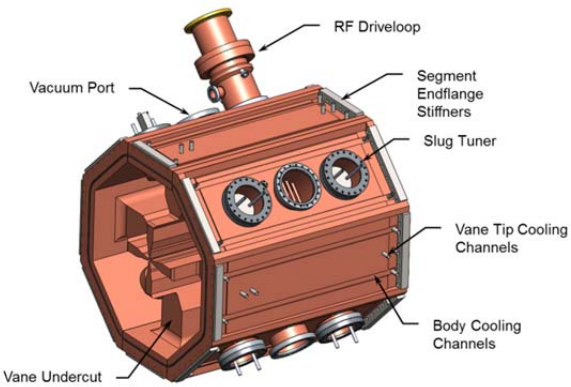

Figure 15: RFQ assembly view of segment 1 with endplate removed.

Mechanical construction of the RFQ will be performed as an integral brazed structure with dual-circuit cooling water resonance control. Overall mechanical fabrication is performed in 5 longitudinal sections to minimize machining and handling weight. The quadrupole and dipole mode frequencies are fine-tuned during construction using fixed mechanical slug tuners in all 4 quadrants distributed along the length of the machine. Dipole mode suppression rods attached to the structure endplates are utilized to separate and move dipole mode frequencies away from the accelerating mode frequency, thus stabilizing the desired quadrupole accelerating mode at 80.5 MHz. The field ramp in the accelerating mode is accomplished through proper sizing of the magnetic return vane undercuts at the ends of the structure and power is fed using a magnetic-field loop-coupler drive.

Thermal management of CW RFQ's is challenging but given the modest drive power of below 100 kW, no significant cooling issues exist. All components are made of high-conductivity copper and actively water cooled: resonator vanes, endplates, slug tuners, vacuum pumping port grills and the 15.6-cm diameter coaxial drive coupler power feed. Additional care is taken in the vane-undercut regions where the local RF heating is increased due to magnetic-field compression in these zones.

Magnet and Power Supply

Most of the magnets in the driver linac are resistive due to the relatively low beam rigidity. Superconducting dipoles are used when fields of 2 T are required (folding segment 2). The fragment separator uses SC technology to allow the high pole-tip fields and large apertures required to maximize the acceptance. Re-configuration of the existing A1900 fragment separator allows connection to the existing NSCL experimental equipment.

Power supplies are largely in three categories, room-temperature magnet power supplies, SC magnet power

supplies, and high-voltage power supplies. Programmable power supplies provide regulated DC current to the magnets, or regulated high voltage to electrostatic elements and ion source components.

Diagnostics

The driver linac is planned to be commissioned with single-shot or low repetition rate, 50 μA and 50 μs beam pulses. This sets the fundamental operating specification for most diagnostics systems. In full operation, the diagnostics must accommodate low-to-moderate energy, low instantaneous current, CW, high-power beams of differing ion species with high charge states.

Use of intercepting diagnostic devices is acceptable only under tightly controlled, low-beam-power conditions and only at locations not adjacent to SC cavities. Also, FRIB low-energy, heavy-ion beams do not avail themselves to many optical diagnostics techniques used for highly-relativistic beams. Beam position and beam current monitoring system design is challenged by the continuous, low-current (500 μA maximum) nature of the FRIB beam. The present specification for the operational "CW" beam includes a 50 μs beam gap at 100 Hz primarily for diagnostics purposes.

The FRIB beams present particular challenges for beam loss monitoring, which is traditionally expected to provide important signals for machine protection and for beam tuning and optimization. Full loss of the CW heavy ion beam, even at relatively low energies, can cause component damage in tens of microseconds. At low energies, e.g. all of LS1, the radiation signature outside the beam line elements can be vanishingly small. Distributed, chronic, fractionally small losses of the CW beam can adversely load the cryogenic system. Radiation cross-talk between adjacent segments of the folded FRIB linac configuration is large [4]. Finally, there is expected to be a competing radiation field due to X-rays from SRF cavities, which is yet to be quantified.

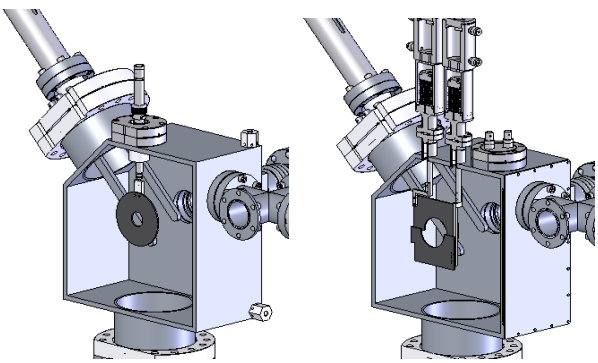

Figure 16: Standardized accelerator vacuum chambers with diagnostics ports. Also shown are fixed (left) and variable (right) diameter halo scrapers for interceptive beam-loss monitoring.

Aperture-limiting "halo rings", instrumented to sense the deposited charge, are being considered for monitoring chronic, small beam losses [4]. The halo rings would be located in the warm, inter-cryomodule regions. Conceptual designs for fixed- and adjustable-aperture halo rings are shown in Figure 16.

Vacuum and Alignment

Beam-boxes as shown in Figure 16 of two standardized lengths and identical diagnostics ports will be installed across the entire driver accelerator. Over 100 ion pumps are used to generate vacuum ranging from 10^{-6} Torr (charge-stripping section) to $5x10^{-9}$ Torr (warm region between cryomodules). Vacuum requirements are primarily determined by the need to minimize stripping of the highly-charged heavy ions. Effects of electron cloud are expected to be negligible. The Molflow+ codes [22] are used to guide the pump sizing and placements.

Planning for the alignment of the facility is underway. In the near-term we focus on designing the alignment network including characterization of the existing network in the NSCL facility matching the FRIB global-coordinate system. The alignment network encompasses the front end beam lines at ground level, a 10-m vertical drop to the over 3,066 m^2 linac tunnel, heavily shielded target system chambers, and a vertical rise back to and including the entire existing NSCL facility.

Weight and structural analysis and differential-settlement monitoring is included as part of conventional-facility design.

Controls

As the interface for operators and physicists to commission and operate the FRIB accelerator, the control system provides supervisory and model-driven control (Table 4).

Table 4: FRIB distributed control system.

Physical Distribution	~200 m * 200 m
IOCs	~150 Computers/EPICS Input/Output Controllers (IOC)
PLCs	~100 Programmable Logic Controllers (PLC)
Network	~ 3000 GbE ports
Global Timing	>500 timing drop points
Machine Protection	~2000 MPS fast protection inputs
Conventional Facility	~760 racks and more than 100 with controls devices

The low-level control system consists of programmable-logic-controllers (PLC), input-output-controllers (IOC) and signal-conditioning modules to provide process control and remote operation to the field devices including vacuum devices, power supplies, RF controllers and cryogenic sensors/controllers.

The global system provides site-wide timing (event and data), network connectivity and integration of machine protection to allow all subsystems to work together with synchronized real-time information, Ethernet-based communication and consistent fault handling. The machine mode, beam mode and particle type are first set in global system and then distributed throughout the facility to ensure that every related subsystem has consistent information.

The high-level applications provide both web- and console-based operation toolkits, relational-database services and model-based physics applications to support installation, commissioning and operations. The service-oriented architecture is selected, the key technologies such as Eclipse/CSS, J2EE, XAL and MySQL are decided and a set of tools are developed.

Utilities

A robust infrastructure is designed to support FRIB accelerator operations including facility power, cooling water, air, cable trays and conduits, facility layout and grounding.

The FRIB facility will be served by two 25 MW, 13.8 kV primary feeders from the MSU T.B. Simon Power Plant using an automatic transfer arrangement to transfer load in the event of a circuit failure. The feeders are installed in an underground duct bank providing protection from foreseeable hazardous weather. An additional 4 MW, 13.8 kV primary feeder is also routed to the site to serve as investment protection in the unlikely scenario that both primary feeders are lost. This 4-MW feeder requires manual operation to energize and serve loads associated with cryogenics operations. These three circuits serve a line-up of medium-voltage 15 kV switches in a loop configuration with multiple tie-switches offering flexibility in transporting power to various substations throughout the facility. Critical loads that cannot tolerate a power failure such as control equipment for cryogenics, communications, oxygen-deficiency-hazard (ODH) monitoring, personnel and safety protection systems are served by three 200 kW (N+1) uninterruptible power supplies (UPS). The UPS's will maintain power to the critical loads while two 800-kW diesel generators operating in parallel come on-line to provide power to the critical, emergency, legally required standby, and optional standby loads and the fire pump. A facility grounding plan was developed that minimizes conducted and radiated electromagnetic interferences. Ground mesh and mechanical bonding are strategically located to optimize effectiveness [23].

FRIB driver accelerator's electrical components will be housed in 768 racks in the service building. The racks are organized in 120 groups that follow the contour of the accelerator. Conduit banks are located near each rack group to keep cable lengths as short as possible. There are 1200 conduits in these banks that carry electrical signals from RF, power supplies, diagnostics, and controls in the accelerator tunnel. The conduits are 6-m long, and nominal cable lengths are about 30-m long. Thermal modelling is being performed for cable heating in the conduits. The conduits are organized for each rack grouping by RF, DC power supply leads, high voltage, controls, personnel-protection system (PPS), and AC power distribution for cryogenic heaters.

Three primary water cooling loops are specified for the accelerator systems' technical equipment. An activated low-conductivity-water (LCW) system supplies the equipment in the accelerator tunnel while a non-activated LCW system supplies the Front End systems. These are nominally 3-MΩ systems at 32˚C supply temperature incorporating oxygen reducing system and ultra-violet (UV) control of biological growth. Service building rack cooling is accomplished using filtered, treated water since LCW is not required.

Instrument-grade compressed air is routed throughout the facility for the operation of control valves and solenoids, as well as for blowing out water lines and magnets during maintenance.

Heating, ventilation, and air-condition (HVAC) system loads and type are specified for all areas of the facility. Fan-coil units which are supplied by hot and cold water systems are located throughout the accelerator tunnel. These units provide the primary air temperature management during operation. A negative (5 mbar sub-atmospheric) tunnel pressure during operation is provided via a 142 m^3/min exhaust system venting through an exhaust gas management system with make-up air being pre-conditioned through a conventional HVAC unit. Service building rack area cooling is via a raised floor "server room" style cooling system. Air will be supplied at 13˚C through the floor and ducted to racks as needed.

Ground vibration may induce movement in the SC cavities, disrupting the beam and demanding increased RF power. The warm-gas compressors of the helium refrigeration system are a major concern, especially since the system is planned to be housed adjacent to the service building above the tunnel to save conventional-construction costs. Studies concluded that the compressor vibration can be adequately mitigated by mechanically isolating compressors using commercially-available foundation pads [24]. The effects from other equipment like cooling-water pumps and chillers also are assessed and comparable vibration-reduction measures implemented.

FUTURE PERSPECTIVES

The FRIB accelerator design is advanced towards beginning construction in 2014. Early procurements before 2014 is strategically planned to establish the front end test stand to demonstrate critical components of the ECR ion source and the fully powered RFQ, to contract on long lead-time cryogenic refrigeration subcomponents, to acquire cryogenic distribution equipment that needs to be installed before accelerator tunnel completion, and to acquire SRF components to be assembled in the pre-production cryomodules. Upon fabrication, installation, and integrated tests, early beam commissioning is expected to be staged from 2017 to 2019. The facility is scheduled to meet key performance parameters supporting routine user operations before 2021. Full design capability is expected to be reached within 4 years after the beginning of routine operations. Science driven upgrade options may be pursued at any stage of the project.

ACKNOWLEDGMENTS

FRIB accelerator systems design has been assisted under work-for-others agreements by many national laboratories including ANL, BNL, FNAL, JLAB, LANL, LBNL, ORNL, and SLAC, and in collaboration with many institutes including BINP, KEK, IMP, INFN, INR, RIKEN, TRIUMF, and Tsinghua University. We thank the Accelerator Systems Advisory Committee chaired by S. Ozaki for their valuable advice and guidance, B. Laxdal, P. Kneisel, and A.C. Crawford for their participation in the FRIB weekly teleconference, colleagues who participated in FRIB accelerator peer reviews including A. Aleksandrov, G. Ambrosio, W. Barletta, G. Bauer, G. Biallas, J. Bisognano, S. Bousson, M. Champion, M. Crofford, R. Cutler, B. Dalesio, G. Decker, J. Delayen, H. Edwards, J. Error, J. Fuerst, K. Kurukawa, J. Galambos, J. Galayda, J. Gilpatrick, S. Gourlay, S. Henderson, L. Hoff, G. Hoffstaetter, J. Hogan, N. Holtkamp, H. Horiike, C. Hovater, H. Imao, R. Janssens, R. Keller, J. Kelley, P. Kelley, M. Kelly, J. Kerby, A. Klebaner, J. Knobloch, J. Mammosser, T. Mann, N. Mokhov, G. Murdoch, H. Okuno, P. Ostroumov, R. Pardo, S. Peggs, T. Peterson, C. Piller, J. Power, T. Powers, J. Preble, D. Raparia, T. Roser, R. Ruland, W.J. Schneider, D. Schrage, J. Sondericker, W. Soyars, C. Spencer, R. Stanek, M. Stettler, J. Stovall, V. Verzilov, P. Wanderer, M. Wiseman, L. Young, and A. Zaltsman, and colleagues who advised and collaborated with the FRIB team including A. Burrill, K. Davis, W. Hartung, A. Hutton, R. Kersevan, S.H. Kim, K. Macha, G. Maler, E.A. McEwen, W. Meng, T. Reilly, J. Sandberg, J. Tuozzolo, and J. Vincent. At Michigan State University, the FRIB accelerator design is executed by a dedicated team of the FRIB Accelerator Systems Division with close collaboration with the Experimental Systems Division headed by G. Bollen, the Conventional Facility Division healed by B. Bull, the Chief Engineer's team headed by D. Stout, and supported by the project controls, procurements, ES&H of the FRIB Project, by the NSCL, and by the MSU.

REFERENCES

[1] Web site http://www.frib.msu.edu/
[2] D. Leitner et al, "Status of the ReAccelerator Facility RεA for Rare Isotopes beam research", SRF'2011, Chicago (2011, in press).
[3] J. Wei, Rev. Mod. Phys., 75, (2003) 1383.
[4] Z. Liu, Y. Zhang et al, "Ion Chambers and Halo Rings for Loss Detection at FRIB", IPAC'12, New Orleans (2012, in press).
[5] Y. Zhang, "Beam Tuning Strategy of the FRIB Linac Driver"; P. Chu et al, "Online Physics Model Platform", IPAC'12, New Orleans (2012, in press).
[6] N. Holtkamp, "The SNS Linac and Storage Ring: Challenges and Progress Towards Meeting Them", EPAC'02, Paris, p. 164.
[7] X. Wu et al, "The Overview of the Accelerator System for the Facility for Rare Isotope Beams at Michigan State University, LINAC'10, Tsukuba, p. 163; Q. Zhao et al, "Beam Dynamics in the FRIB Linac", HB'12, Beijing (2012, to be published).
[8] F. Marti et al., "Development of Stripper Options for FRIB", LINAC'10, Tsukuba, p. 662.
[9] R. Ronningen et al, Nucl. Tech., 168 (2009) 670.
[10] T. Roser, private communications.
[11] Y. Momozaki et al., JINST 4 (2009) P04005.
[12] H. Okuno et al., Phys. Rev. ST Accel. Beams, 14, (2011) 033503.
[13] C. Compton et al., "Superconducting Resonators Production for Ion Linacs at Michigan State University", SRF'11, Chicago (2012, in press).
[14] A. Facco et al, "Superconducting Resonators Development for the FRIB and ReA Linacs at MSU: Recent Achievements and Future Goals", IPAC'12; J. Popielarski et al., "Dewar Testing of Coaxial Resonators at Michigan State University", IPAC'12, New Orleans (2012, in press).
[15] L. Popielarski et al., "Cleanroom Techniques to Improve Surface Cleanliness and Repeatability for SRF Coldmass Production", IPAC'12, New Orleans (2012, in press).
[16] D. Leitner et al, Rev. Sci. Instru. 79 (2008) 02C710.
[17] M. Leitner, "Design Status of the SRF Linac Systems for the Facility for Rare Isotope Beams", SRF'11, Chicago (2011, in press).
[18] V. Ganni, "Helium Refrigeration Considerations for Cryomodule Design," Proc. ADS Conf., Mumbai (2011, in press).
[19] P. Knudsen, V. Ganni, "Process Options for Nominal 2-K Helium Refrigeration System Designs", Adv. Cryo. Eng. 57, AIP, New York (2012, in press).
[20] V. Ganni, P. Knudsen, "Optimal Design and Operation of Helium Refrigeration Systems Using the Ganni Cycle," Adv. Cryo. Eng. 55, AIP, New York (2010) p. 1057.
[21] M. Johnson et al, "Design of the FRIB Cryomodule", IPAC'12, New Orleans (2012, in press).
[22] Codes Molflow+, R. Kersevan, CERN.
[23] M. Thuot, "Using the FRIB Facility Grounding Mesh Effectively", FRIB Internal Document T10503-VS-000001 (2012); D. Stout et al, "201105 Grounding Workshop Report", FRIB Internal Document T20100-RA-000043 (2011).
[24] H. Amick, "Review of Ground-Borne Vibration Issues", FRIB Internal Document T20201-TD-000082 (2011); J.A. Moore, E. E. Ungar, FRIB Internal Document T20201-TD-000083 (2011); D. Stout et al, "FRIB Ground-Born Vibration Studies", FRIB Internal Document T31200-TD-000084 (2011).